AMERICAN SOCIETY FOR MICROBIOLOGY | Antimicrobial Agents and Chemotherapy®

Exploring Ubiquinone Biosynthesis Inhibition as a Strategy for Improving Atovaquone Efficacy in Malaria

I. B. Verdaguer,[a] M. Crispim,[a] C. A. Zafra,[a] R. A. C. Sussmann,[b] N. L. Buriticá,[a] H. R. Melo,[c] M. F. Azevedo,[c] F. G. Almeida,[a] E. A. Kimura,[a] A. M. Katzin[a]

[a]Department of Parasitology, Institute of Biomedical Sciences, University of São Paulo, São Paulo, Brazil
[b]Center for Environmental Sciences, Institute of Humanities, Arts and Sciences, Federal University of Southern Bahia, Itabuna, Brazil
[c]Department de Bioscience, Federal University of São Paulo, São Paulo, Brazil

Ignasi Bofill Verdaguer and Marcell Crispim contributed equally to this work. Author order was determined by drawing straws.

ABSTRACT Atovaquone (AV) acts on the malaria parasite by competing with ubiquinol (UQH_2) for its union to the mitochondrial bc_1 complex, preventing the ubiquinone-8 and ubiquinone-9 (UQ-8 and UQ-9) redox recycling, which is a necessary step in pyrimidine biosynthesis. This study focused on UQ biosynthesis in *Plasmodium falciparum* and adopted proof-of-concept research to better elucidate the mechanism of action of AV and improve its efficacy. Initially, UQ biosynthesis was evaluated using several radioactive precursors and chromatographic techniques. This methodology was suitable for studying the biosynthesis of both UQ homologs and its redox state. Additionally, the composition of UQ was investigated in parasites cultivated at different oxygen saturations or in the presence of AV. AV affected the redox states of both UQ-8 and UQ-9 homologs by increasing the levels of the respective reduced forms. Conversely, low-oxygen environments specifically inhibited UQ-9 biosynthesis and increased the antimalarial efficacy of AV. These findings encouraged us to investigate the biological importance and the potential of UQ biosynthesis as a drug target based on its inhibition by 4-nitrobenzoate (4-NB), a 4-hydroxybenzoate (4-HB) analog. 4-NB effectively inhibits UQ biosynthesis and enhances the effects of AV on parasitic growth and respiration rate. Although 4-NB itself exhibits poor antimalarial activity, its 50% inhibitory concentration (IC_{50}) value increased significantly in the presence of a soluble UQ analog, *p*-aminobenzoic acid (pABA), or 4-HB. These results indicate the potential of AV combined with 4-NB as a novel therapy for malaria and other diseases caused by AV-sensitive pathogens.

KEYWORDS *Plasmodium falciparum*, malaria, ubiquinone, biosynthesis, oxygen levels, atovaquone, 4-nitrobenzoate, antimalarial agents

Malaria is a neglected parasitic disease that is endemic in Africa, South Asia, and South America, and its eradication involves biological, financial, and institutional challenges (1, 2). In 2018, 228 million people suffered from malaria and more than 400,000 deaths were recorded, most of them children under 5 years of age. The majority of deaths that occurred in Africa were due to *Plasmodium falciparum* infections. Several cases of drug resistance have been reported (1); hence, new antimalarial therapies are necessary. The use of combination therapies has become one of the most common strategies to avoid the spread of drug resistance (3).

The mitochondrion in *Plasmodium* species is considered one of the most promising drug targets (4). This organelle is functionally active at different oxygen levels and is believed to adapt its roles at different parasitic stages (5, 6). The organelle possesses different ubiquinone-dependent dehydrogenases: a rotenone-insensitive NADH dehydrogenase, dihydroorotate dehydrogenase (DHODH), glycerol 3-phosphate dehydrogenase, succinate dehydrogenase, and the malate quinone oxidoreductase (7, 8) (Fig. 1). Atovaquone

Citation Verdaguer IB, Crispim M, Zafra CA, Sussmann RAC, Buriticá NL, Melo HR, Azevedo MF, Almeida FG, Kimura EA, Katzin AM. 2021. Exploring ubiquinone biosynthesis inhibition as a strategy for improving atovaquone efficacy in malaria. Antimicrob Agents Chemother 65:e01516-20. https://doi.org/10.1128/AAC.01516-20.

Address correspondence to A. M. Katzin, amkatzin@icb.usp.br.

Received 15 July 2020
Returned for modification 18 September 2020
Accepted 16 January 2021
Accepted manuscript posted online 25 January 2021
Published 18 March 2021

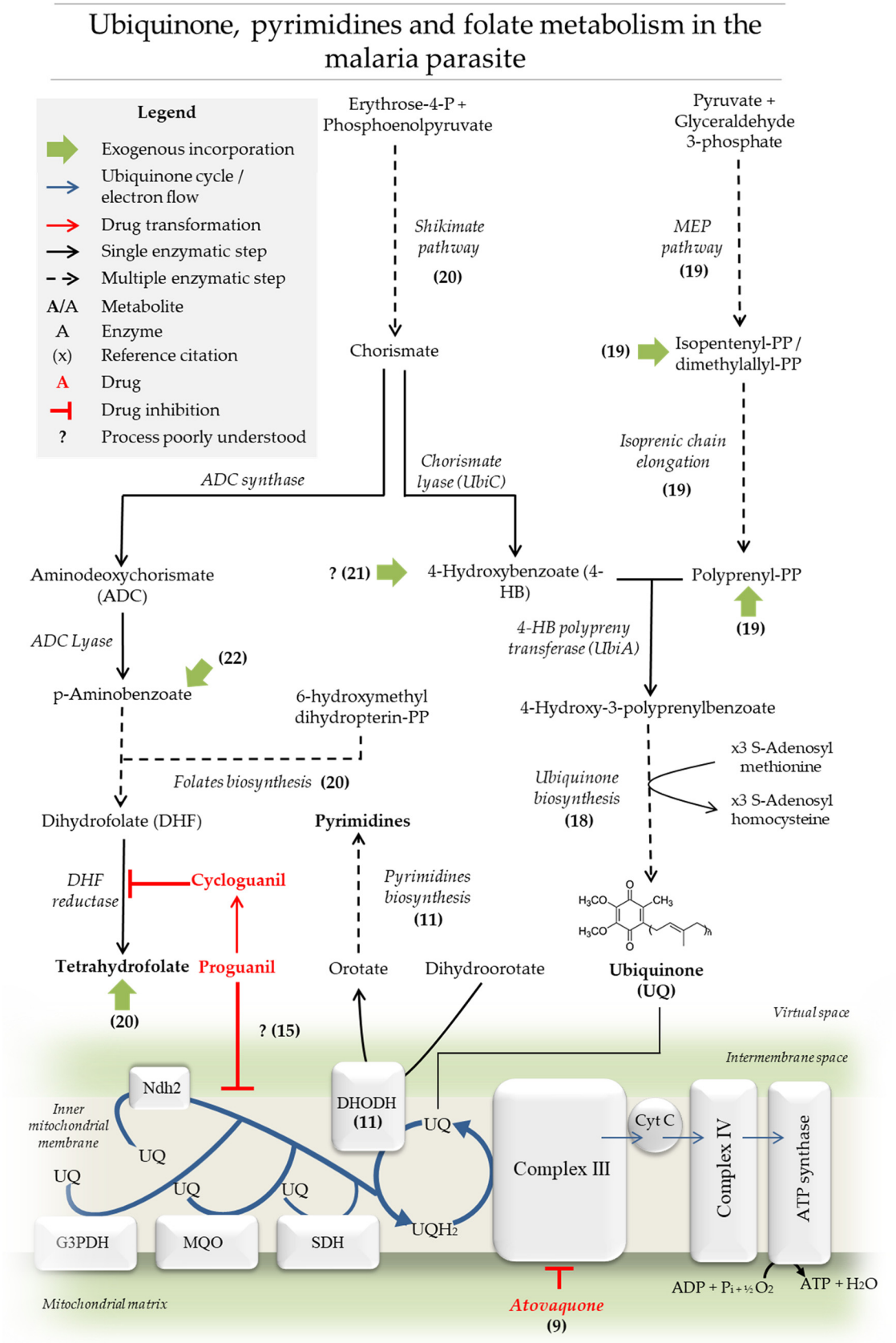

FIG 1 Ubiquinone, pyrimidines, and folate metabolism in the malaria parasite. Schematic representation of UQ, folate, and pyrimidine biosynthetic pathways as well as the specific role of UQ in the mitochondrial electron transport system in *Plasmodium*.

(Continued on next page)

(AV, *trans*-2-[4-(4-chlorophenyl)cyclohexyl]-3-hydroxy-1,4-naphthalenedione) collapses mitochondrial membrane potential in the parasite, and its clinical effectiveness in malaria and other infectious diseases such as babesiosis, *Pneumocystis jirovecii* infection, and toxoplasmosis has already been reported (9). AV is thought to compete with ubiquinol (UQH_2) for the cytochrome bc_1 complex (8, 9) (Fig. 1). Contrary to what is observed in most organisms, ATP synthesis via oxidative phosphorylation is believed to be nonessential in the asexual stages of the parasite (10). Moreover, AV antiplasmodial activity is reduced significantly in transgenic parasites complemented with the yeast ubiquinone (UQ)-independent DHODH (11). It was concluded that the major lethal effects of AV are attributed to the inhibition of UQ redox regeneration, which is required for pyrimidine biosynthesis. Therefore, it is not surprising that the antiparasitic effects of AV can be rescued upon the exogenous addition of decyl-UQ (dUQ), a soluble analog of UQ (12).

AV administered in isolation appears to have insufficient efficacy in malaria treatment owing to recrudescence and resistance phenomena (13). Therefore, in clinical practice, AV is combined with the prodrug proguanil [1-(4-chlorophenyl)-2-(N′-propan-2-ylcarbamimidoyl) guanidine] and commercially distributed as Malarone. Cycloguanil is a proguanil-derived metabolite which inhibits the enzyme dihydrofolate reductase (DHFR) (14). However, the mechanism by which proguanil enhances AV effects seems to be independent of DHFR inhibition and is likely mediated by proguanil itself rather than cycloguanil (15, 16). Srivastava & Vaidya demonstrated that proguanil enhances the ability of AV to induce the collapse of the mitochondrial membrane potential ($\Delta\Psi$ mt) despite exerting negligible effects on $\Delta\Psi$ mt and respiration rate when used in isolation (15, 16). Unfortunately, parasitic resistance to Malarone has also been demonstrated; moreover, the treatment is considerably expensive and, therefore, inaccessible in most regions where malaria is endemic (17).

As mentioned, the mechanism of action of AV is associated with interference in the UQ-dependent pathways. In *Plasmodium*, the shikimate pathway and the 2-*C*-methyl-D-erythritol 4-phosphate (MEP) pathway are the sources for the biosynthesis of the UQ aromatic head group and isoprenic chain precursors, respectively (18) (Fig. 1). The MEP pathway produces isopentenyl pyrophosphate (IPP) and its isomer dimethylallyl pyrophosphate (DMAPP), the basic 5-carbon isoprenic units. The subsequent condensation of isoprenic units leads to the formation of polyprenyl moieties such as geranyl pyrophosphate (GPP, 10 carbons), farnesyl pyrophosphate (FPP, 15 carbons), geranylgeranyl pyrophosphate (GGPP, 20 carbons) (19), and lengthier isoprene chains.

In several organisms, the shikimate pathway generates chorismate, which in turn can be converted to 4-hydroxybenzoate (4-HB) by chorismate lyase (UbiC; EC 4.1.3.40) for UQ biosynthesis or to *p*-aminobenzoic acid (pABA) by aminodeoxychorismate synthase and aminodeoxychorismate lyase enzymes (ACDS/ACDL; EC 2.6.1.85/EC 4.1.3.38) (Fig. 1) (18, 20). *In vivo* experiments on *Plasmodium gallinaceum* in chicks suggested that the exogenous incorporation of both pABA and 4-HB from the host occurs (21). Furthermore, pABA transport has been well characterized in *P. falciparum*-infected erythrocytes (22).

Once the polyprenyl moieties and 4-HB are available, the specific UQ biosynthesis pathway can be initiated with the prenylation of 4-HB by the enzyme 4-HB polyprenyltransferase (UbiA; EC 2.5.1.39; PF3D7_0607500, putative) (Fig. 1). The product, 3-poliprenyl-4-hidroxybenzoate, undergoes several structural modifications on its aromatic head group (18). These modifications include hydroxylations, a decarboxylation, and *S*-adenosyl-L-methionine (SAM)-mediated methylations catalyzed by the enzymes 2-polyprenyl-6-hydroxyphenyl methylase/3-demethylubiquinone 3-methyltransferase (UbiG/

FIG 1 Legend (Continued)
The biosynthesis of UQ and folates' aromatic precursors by the shikimate pathway are also shown. The MEP pathway generates IPP or DMAPP necessary for the formation of longer isoprenic chains by polyprenyl synthases. The previously mentioned biosynthetic pathways are located in different compartments and thus here are represented in a single virtual space. Finally, the UQ biosynthetic pathway and its function in the mitochondria are indicated. UQ functions as an electron carrier for rotenone-insensitive NADH dehydrogenase (Ndh2), dihydroorotate dehydrogenase (DHODH), glycerol 3-phosphate dehydrogenase (G3PDH), succinate dehydrogenase (SDH), malate quinone oxidoreductase, and mitochondrial complex III.

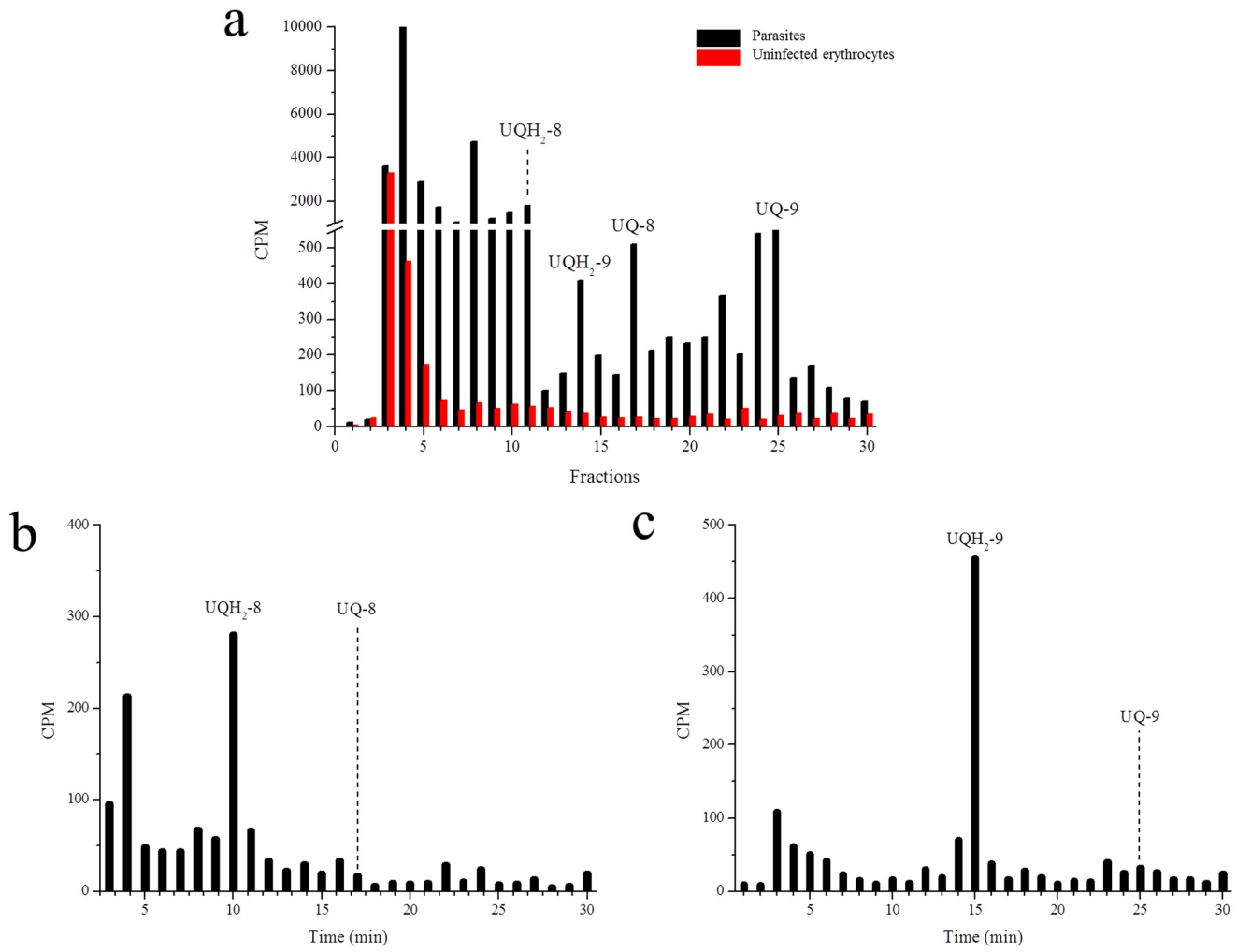

FIG 2 [^{3}H] GGPP incorporation into ubiquinones. (a) RP-HPLC metabolic profiles of erythrocytes uninfected or infected with *P. falciparum* schizonts. Uninfected or infected erythrocytes were incubated with [^{3}H] GGPP. (b and c) UQ-8 (b) or UQ-9 (c) from [^{3}H] GGPP-radiolabeled parasites were purified by RP-HPLC. Both UQ homologs were chemically reduced and analyzed by the same chromatography method. In all experiments, samples were co-injected with UQ standards. The fractions were collected at 1 min. This experiment was performed twice with similar results. UQ-8, ubiquinone-8; UQH_2-8, ubiquinol-8; UQ-9, ubiquinone-9; UQH_2-9, ubiquinol-9.

Coq3; EC 2.1.1.222/2.1.1.64; PF3D7_0724300, putative) and 2-methoxy-6-polyprenyl-1,4-benzoquinol methylase (UbiE, EC 1.14.99.60; PF3D7_0407100, putative) (18). However, there is limited biochemical evidence of UQ biosynthesis in the malaria parasite. Specifically, the detection of *Plasmodium knowlesi*-produced UQ was performed by metabolic labeling with [^{14}C] 4-hydroxybenzoic acid and chromatographic analysis (23). In *P. falciparum*, the incorporations of [^{14}C] 4-hydroxybenzoic acid, [1-^{14}C] sodium acetate, and [^{3}H] isoprenic moieties were reported (24).

In this study, we characterized the physiological behavior of UQs under different conditions and in response to treatment with AV. We also aimed to develop a strategy for the inhibition of UQ biosynthesis and assessed its potential as a drug target.

RESULTS

Ubiquinone homologs identification. Parasitic UQ biosynthesis identification by chromatography was first performed by radiolabeling parasites with [^{3}H] GGPP. The chromatographic system offered a higher resolution than reverse phase-high performance liquid chromatography (RP-HPLC) systems previously used for studying UQs in the malaria parasite by other authors (19, 23, 24). It was confirmed that UQ/UQH_2-8

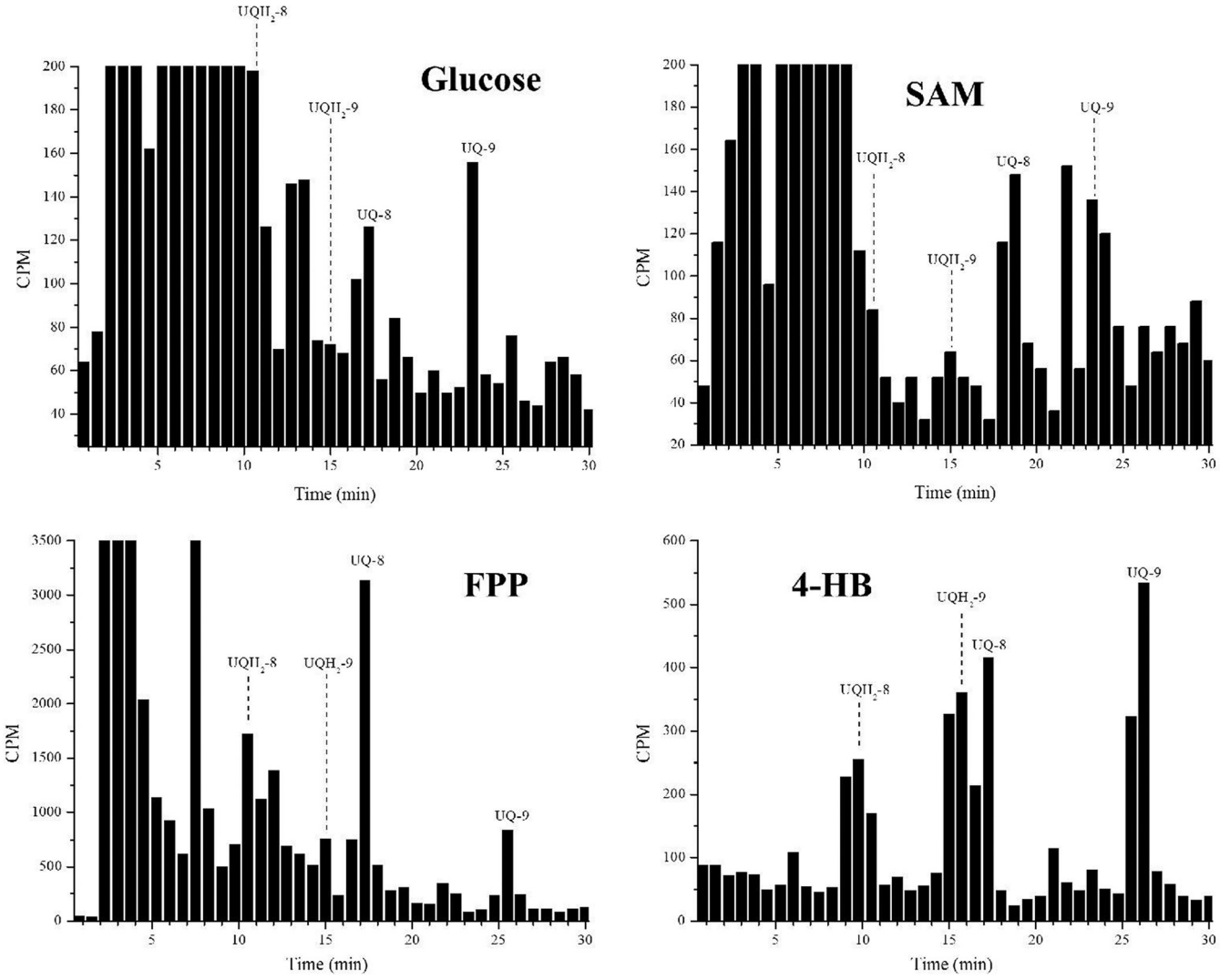

FIG 3 Incorporation of radiolabeled precursors into ubiquinones. RP-HPLC metabolic profiles of erythrocytes infected with *P. falciparum* schizonts incubated with different radiolabeled metabolites, as indicated. In all experiments, the samples were co-injected with UQ standards. The fractions were collected at 0.75 min. Glucose, [^{14}C-U] Glc; SAM, [methyl-^{3}H] SAM; FPP, [^{3}H] FPP; 4-HB, [ring-^{14}C]-4-HB; UQ-8, ubiquinone-8; UQH_2-8, ubiquinol-8; UQ-9, ubiquinone-9; UQH_2-9, ubiquinol-9. These experiments were performed twice for each radiolabeled precursor and all experiments yielded similar results.

eluted at ~17/~10 min and UQ/UQH_2-9 eluted at ~25/~14 min (Fig. 2a). Furthermore, the suitability of this methodology for specific identification of metabolites from the parasite rather than from the host was investigated by radiolabeling uninfected erythrocytes. Labeled UQ was only detected in the infected erythrocytes (Fig. 2 and see Fig. S2 in the supplemental material). Moreover, after the UQs reduction, we observed the displacement of the radioactive signals from the fractions corresponding to each UQ homolog to those fractions corresponding to UQH_2 homolog (Fig. 2b and c and Fig. S2). Therefore, the identity of UQs and the absence of co-elution phenomena with other unsuspected parasitic isoprenylated compounds could be confirmed.

In addition to [^{3}H] GGPP, other radiolabeled precursors were employed. [^{14}C-U] Glc and [ring-^{14}C]-4-HB (Fig. 3 and Fig. S3) appeared to be incorporated better in UQ-9, while [^{3}H] FPP and [methyl-^{3}H] SAM were better incorporated in UQ-8 (Fig. 3 and Fig. S3). The other peak, which appears between UQ-8 and UQ-9, was identified (approximately at 22 min). This peak appears when any of the radiolabeled precursors are employed (including [ring-^{14}C(U)] 4-HB) and probably corresponds to a UQ biosynthesis intermediate.

Prior to this study, the biosynthesis of UQ-8/9 in *P. falciparum* had only been

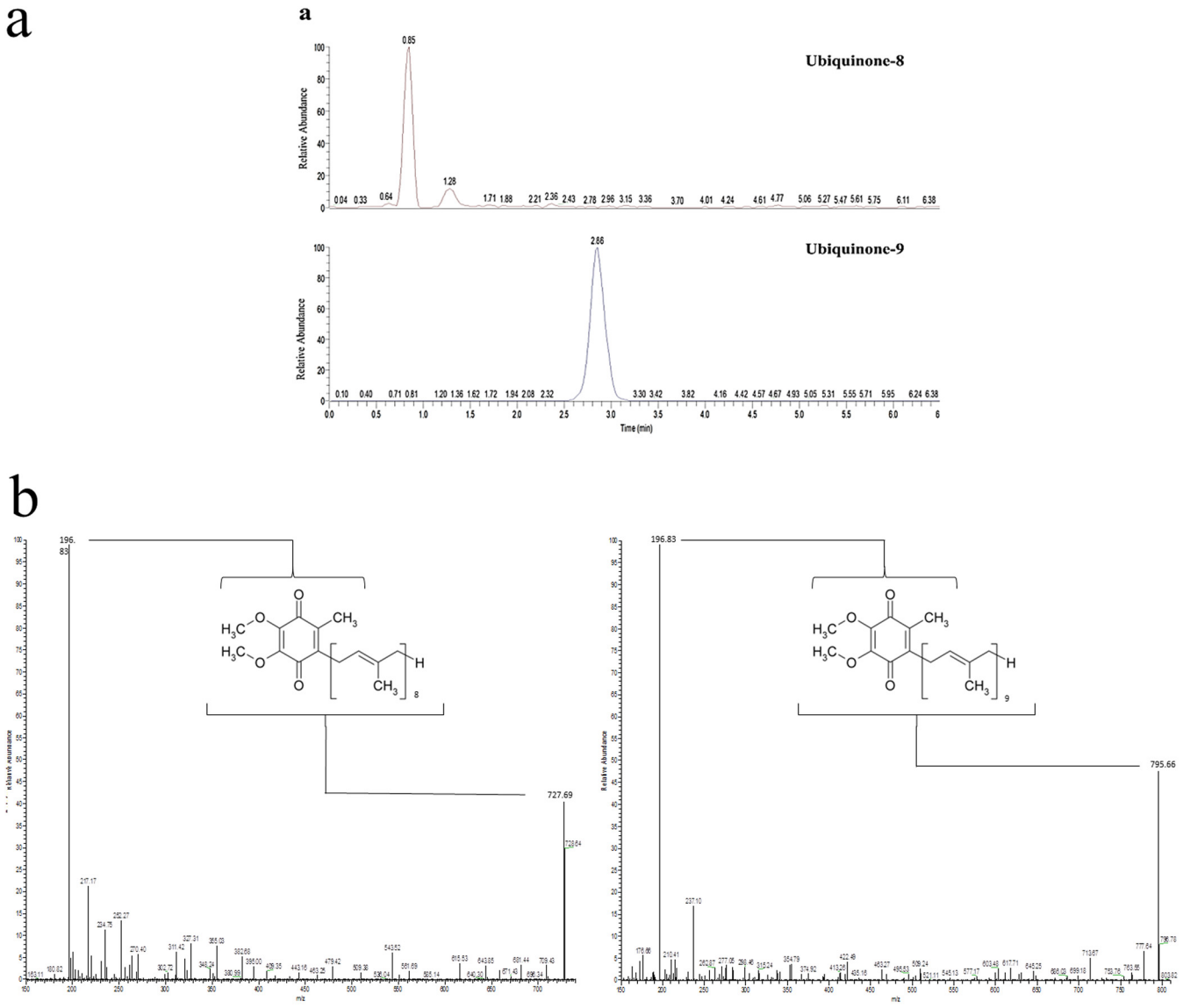

FIG 4 Mass spectrometry analyses. (a) SRM mass spectrometry analysis of 5×10^9 erythrocyte-free parasites. The results show compounds with the same retention time, molecular ion, and break down pattern found in UQ-8/9 standards. (b) Profiles of both UQ-8/9 standards analyzed separately by LC/MS. Ions for both UQ homologs are indicated by the chemical structure of the molecules. This experiment was performed once.

detected by radiolabeling/chromatography (23–25). In this study, the UQs biosynthesized by the parasite were also identified by mass spectrometry (Fig. 4a). The profiles of both UQ-8 and UQ-9 standards were first analyzed separately using LC/MS (Fig. 4b). For the UQ-8 standard, the molecular ion was detected at an *m/z* value of 728. Among the breakdown products, an ion was detected at the *m/z* value of 196.8, which corresponds to the aromatic head group. For the UQ-9 standard, the molecular ion was detected at the *m/z* value of 796. Again, among the breakdown products, an ion was detected at the *m/z* value of 196.8, which corresponds to the aromatic head group. Compounds with the same retention time, molecular ion, and breakdown pattern as those described for the UQ-8/9 standards were identified in the parasite extracts (Fig. 4a).

Changes in ubiquinone biosynthesis at different oxygen levels. UQ-8 biosynthesis remained almost unaffected when parasites were cultured in the oxygen-free gaseous mixture. On the contrary, UQ-9 biosynthesis was reduced due to the lack of oxygen (in the three experiments performed, oxygen-free gaseous mixtures induced at least an ~75% reduction in cpm corresponding to UQ-9 in parasites maintained under

a

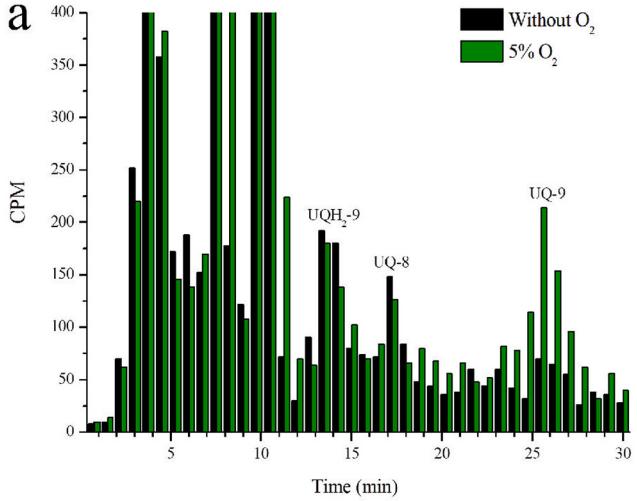

b

Replicate	IC_{50} 5% O_2	IC_{50} Without O_2
1	0.4057	0.287
2	0.5579	0.2774
3	0.5107	0.1612
Mean ± Stdev	0.491 ± 0.078	0.242 ± 0.070***

FIG 5 Effects of oxygen in ubiquinone radioactive incorporation and atovaquone efficacy. (a) RP-HPLC metabolic profiles of [^{3}H] GGPP-radiolabeled *P. falciparum*-infected erythrocytes maintained for 48 h under 5% oxygen or in oxygen-free gaseous mixtures. In all experiments, the samples were co-injected with UQ standards. This experiment was performed thrice with similar results. The fractions were collected at 0.75 min. UQ-8, ubiquinone-8; UQ-9, ubiquinone-9; UQH_2-9, ubiquinol-9. (b) The IC_{50} of AV under oxygen-free or classic gaseous conditions (5% O_2). Results represent the mean of three identical experiments. Results were analyzed by unpaired *t* test in comparison to the control (5% O_2); ***, $P < 0.001$.

classic gaseous conditions), and hence, the total content of biosynthesized UQ was lower (Fig. 5a). No increase in radioactive incorporation was observed in the fractions that were expected to contain both UQH_2 homologs, which suggests that the observed changes were related to UQ biosynthesis rather than a modification of its redox state. Since the UQ pool is reduced under microaerophilic conditions, it was further investigated whether the gaseous composition could affect the efficacy of AV. For this, the parasites were treated with different concentrations of AV and maintained in oxygen-free or in 5% O_2 gaseous mixtures. The IC_{50} values of AV under each condition indicated that the antimalarial agent possess a significantly higher efficacy against parasites maintained in oxygen-poor environments, wherein the UQ content was also lower (Fig. 5b).

AV rescue assays and effects on ubiquinone redox state. We wanted to determine whether only one UQ homolog would be involved in the mitochondrial activity. For this purpose, the parasites were cultured under classic gaseous conditions, radiolabeled with [^{3}H] GGPP, and purified using a magnetic column. The infected erythrocytes were divided into two samples which were suspended and incubated in culture medium or culture medium plus 10 nM AV at 37°C for 10 min. Both samples were then centrifuged; the prenylquinones were extracted from the pellet of infected erythrocytes and chromatographed immediately. The results revealed that AV treatment modified the UQ/UQH_2 ratio by reducing the radioactivity corresponding to UQ-8/9 and increasing the levels of both UQH_2 homologs (in the three experiments performed,

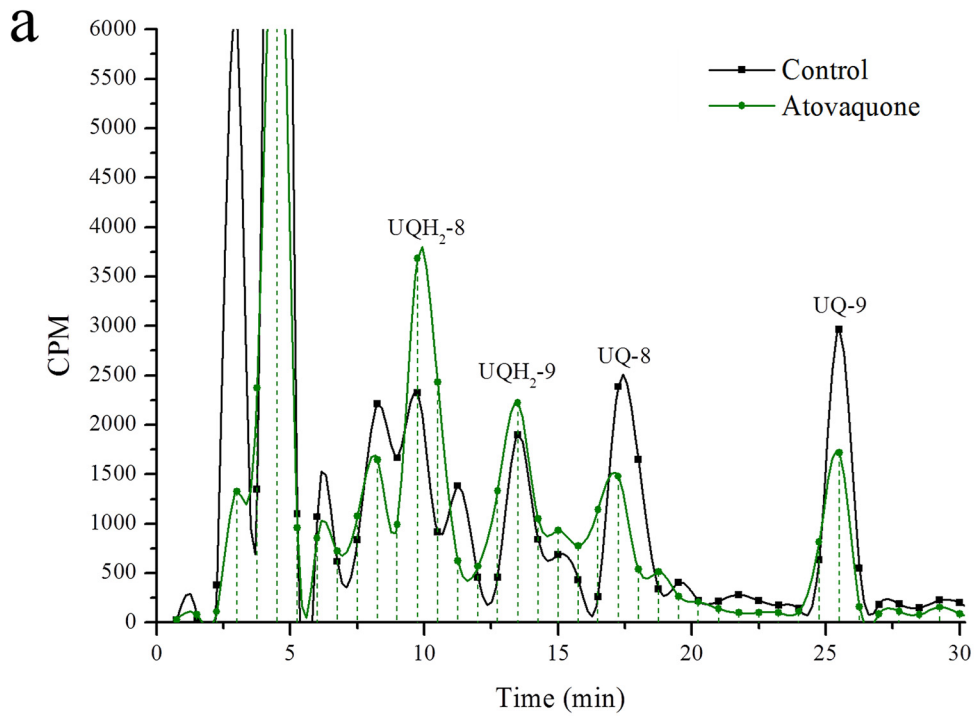

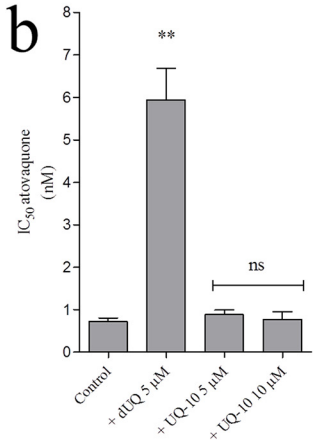

c

	IC_{50} Atovaquone (picomolar)	*p* value
Control	727.00 ± 140.01	-
+ dUQ 5 µM	5944.33 ± 1286.61	0.0022
+ UQ-10 5 µM	891.00 ± 177.67	ns
+ UQ-10 10 µM	776.66 ± 307.38	ns

FIG 6 Effects of atovaquone on ubiquinone redox state and atovaquone rescue assays. (a) RP-HPLC of UQ and UQH_2 labeled with [^{3}H] GGPP in AV untreated/treated parasites. The fractions were collected at 0.75 min. This experiment was performed three times with similar results. UQ-8, ubiquinone-8; UQH_2-8, ubiquinol-8; UQ-9, ubiquinone-9; UQH_2-9, ubiquinol-9. (b and c) IC_{50} values of AV in the presence or absence of 10 μM or 5 μM ubiquinone 10 (UQ-10) or 5 μM decyl-UQ (dUQ) (mean of three identical experiments). The results were studied by unpaired *t* test with respect to the control. *, $P < 0.05$, **, $P < 0.01$, ***, $P < 0.001$.

AV treatment reduced the UQ/UQH_2 cpm ratio from ~1.55 to ~0.77 for UQ-8 and from ~0.9 to ~0.43 for UQ-9) (Fig. 6a).

In another experiment, the AV IC_{50} value was determined when parasites were cultured in the presence or absence of 10 μM or 5 μM dUQ or UQ-10 (Fig. 6b and see Fig. S4 in the supplemental material). At 5 μM, dUQ significantly increased AV IC_{50} value (by approximately 8-fold). It was not possible to calculate AV IC_{50} at 10 μM dUQ since parasites were not killed by any AV concentration tested (Fig. 6b and c; the highest AV concentration tested was 106 nM). Finally, UQ-10 did not affect AV IC_{50} value.

Effects of 4-NB on parasitic growth and ubiquinone biosynthesis. The use of a UQ biosynthesis inhibitor was considered a potential biochemical strategy to explore the dependence of AV efficacy on UQ biosynthesis. 4-NB is a 4-HB analog, which has already been shown to decrease UQ biosynthesis in different organisms, possibly by

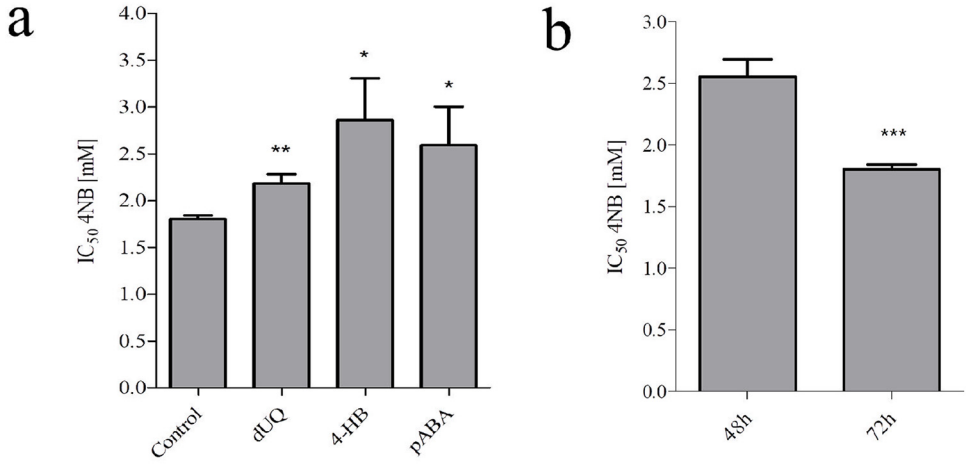

c

	Mean IC_{50} 4-NB (mM)	Mean R^2	*p* value
4-NB 48h	2.555 ± 0.142	0.965 ± 0.002	0.0009
4-NB 72h	1.804 ± 0.038	0,927 ± 0,055	

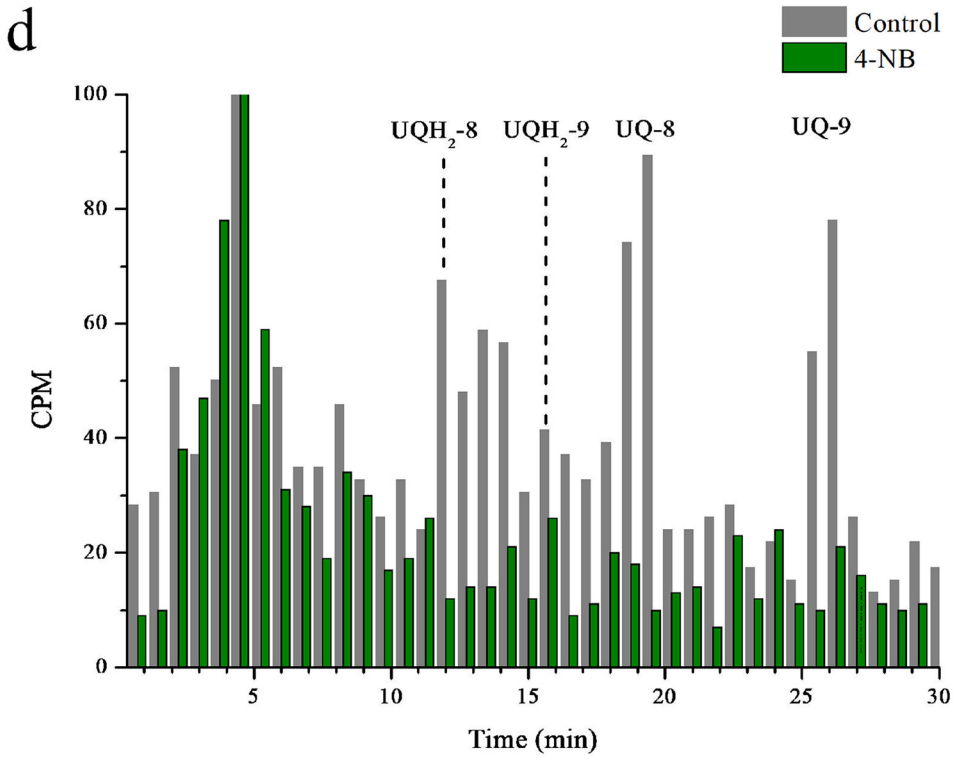

FIG 7 Effects of 4-nitrobenzoate on parasitic growth and ubiquinone biosynthesis. (a) 4-NB IC_{50} value at 72 h indicated by bar graphs showing its deviation in the presence of different compounds (mean of three identical experiments). IC_{50} assays for 4-nitrobenzoate (4-NB) were performed at 72 h and in the presence of 10 μM decyl-UQ (dUQ), 0.5 mM 4-hydroxybenzoate (4-HB), or 0.5 mM *p*-aminobenzoic acid (pABA) (mean of three experiments). (b and c) 4-NB IC_{50} value at 48 and 72 h (mean of three experiments). The data were analyzed using unpaired *t* test in comparison to the untreated control. *, $P < 0.05$, **, $P < 0.01$, ***, $P < 0.001$. (d) RP-HPLC metabolic profiles of [^{3}H] GGPP-radiolabeled *P. falciparum*-infected erythrocytes untreated/treated with 4-NB 1 mM for 48 h. In all experiments, the samples were co-injected with UQ standards. The fractions were collected at 0.75 min. UQ-8, ubiquinone-8; UQH_2-8, ubiquinol-8; UQ-9, ubiquinone-9; UQH_2-9, ubiquinol-9. This experiment was performed twice with similar results.

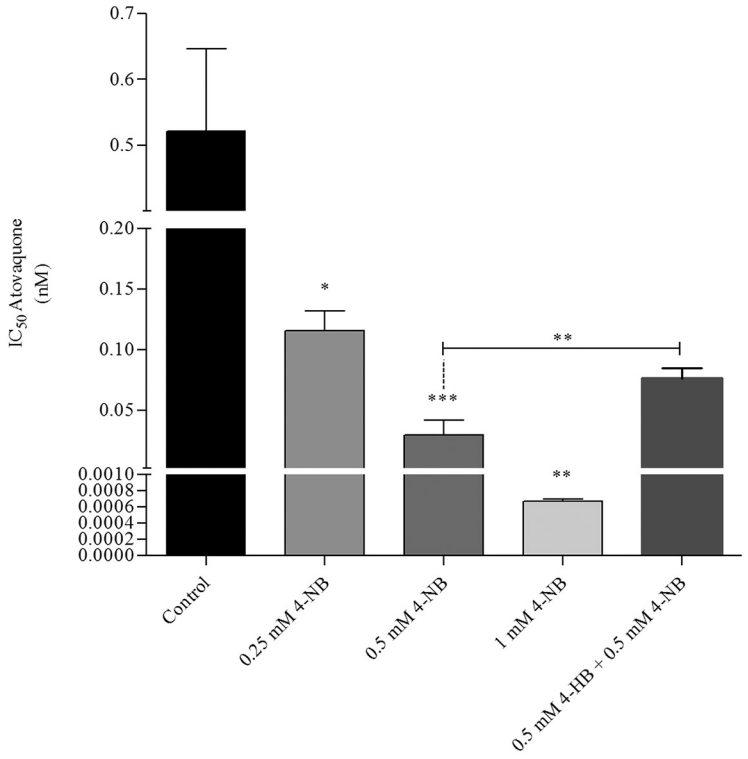

Assay identification	Compound added	IC_{50} Atovaquone ± SD (picomolar)	FIC Atovaquone
A	-	521.74 ± 124.44	-
B	0.25 mM 4-NB	115.45 ± 16.76	0.2213
C	0.5 mM 4-NB	29.65 ± 12.07	0.0568
D	1 mM 4-NB	0.67 ± 0.029	0.0013
E	0.5 mM 4-NB + 0.5 mM 4-HB	76.19 ± 8.75	0.1460

FIG 8 4-Nitrobenzoate enhances atovaquone efficacy. AV IC_{50} values (mean of three identical experiments with four technical replicates each). Assays were performed at 48 h in the presence of 1, 0.5, or 0.25 mM 4-nitrobenzoate (4-NB) or 0.5 mM 4-NB + 0.5 mM 4-hydroxybenzoate (4-HB). In the table, the individual FIC values for AV are presented. The results are depicted by bars that indicate the deviations. Results were analyzed by one-way analysis of variance (ANOVA)/Dunnet's multiple comparison test. *, $P < 0.05$, **, $P < 0.01$, ***, $P < 0.001$.

inhibiting UbiA enzymes (26–28). In *P. falciparum*, 4-NB was observed to have a lower IC_{50} value at 72 h (IC_{50} 1.8 mM) than at 48 h (IC_{50} 2.5 mM) (Fig. 7a, b, and c). In both cases, the results adjusted to a dose-response pattern (Fig. 7c and Fig. S5 and S6). In another experiment, the IC_{50} value of 4-NB was calculated under 10 μM dUQ, 0.5 mM pABA, or 0.5 mM 4-HB. At these concentrations of 4-HB, pABA, and dUQ, no effect on parasitic growth was observed for at least 72 h. The additions of these compounds significantly increased the 4-NB IC_{50} value at 72 h (Fig. 7a). These results indicate that the mechanism underlying the action of 4-NB may involve the competition with 4-HB for UQ biosynthesis or with pABA for folates. The same rescue phenomenon was not observed at 48 h (data not shown). Using radiolabeling methodologies, we further investigated whether 4-NB inhibited UQ biosynthesis. For this, the parasites were radiolabeled with [^{3}H] GGPP while they were cultured in the presence or absence of 1 mM 4-NB (Fig. 7d). The results revealed that 4-NB treatment reduced [^{3}H] GGPP incorporation into both UQ homologs in comparison to that in untreated parasites (in the two experiments performed, 4-NB induced ~80% and ~85% reduction in cpm for UQ-8 and UQ-9, respectively). The concentration of 4-NB selected by us was 1 mM, as it inhibits parasitic growth only by ~5% after 48 h of treatment (Fig. S5 and S6).

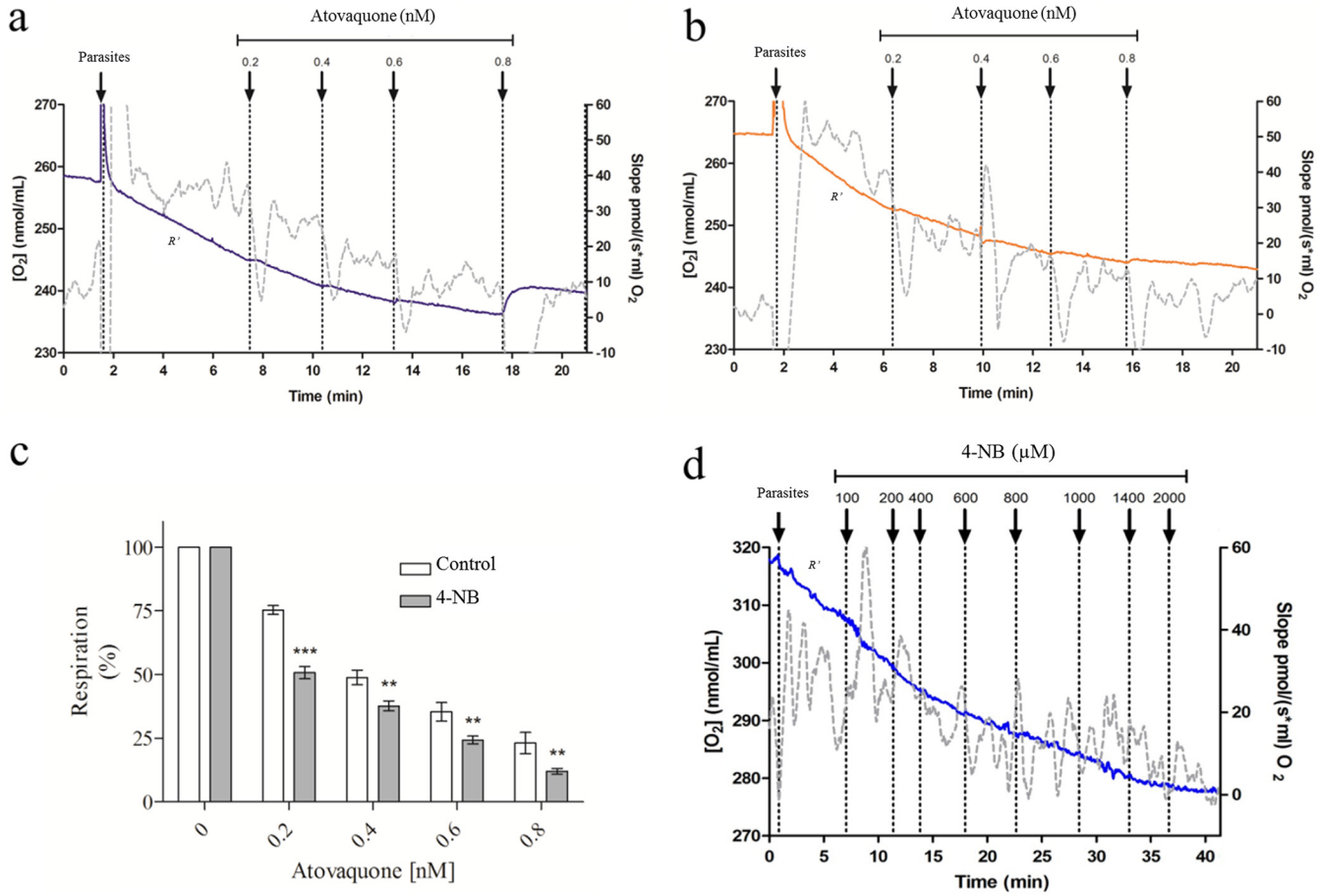

FIG 9 Respiratory rates in erythrocyte-free parasites. Oxygen consumption was measured in erythrocyte-free parasites. The gray lines indicate the slope variation of oxygen concentration as a function of time (right axis). The blue and orange lines represent O_2 concentration (left axis). (a) As a positive control, the parasites were maintained in respiratory buffer. (b) Cultures were treated for 48 h with 4-nitrobenzoate (4-NB). Then, progressive AV doses were added to samples a and b. (c) Respiration percentage: the respiration slopes at specific AV concentrations were normalized by the corresponding R′ slope. Results were analyzed by one-way ANOVA followed by Tukey's posttest in comparison to the respective control. ***, $P < 0.001$; *, $P < 0.05$. (d) Erythrocyte-free parasites were treated with progressive 4-NB concentrations. R′, total cellular oxygen consumption. All experiments mentioned here were performed at least thrice with similar results.

4-NB enhances AV efficacy. Once the inhibitory effect of 4-NB on UQ biosynthesis was characterized, its pharmacological relationship with AV was further investigated. For this purpose, AV IC_{50} was calculated while adding different concentrations of 4-NB ranging from 1 to 0.125 mM in RPMI complete medium (see Fig. 8 and Fig. S5 and S6). All the concentrations of 4-NB used here yielded AV fractional inhibitory concentration (FIC) values <0.5. At 1 mM 4-NB, the AV IC_{50} value could be reduced by more than 1,000-fold. Notably, the results revealed the ability of 4-NB to enhance AV efficacy even at concentrations at which the compound did not affect parasitic growth (0.5 to 0.125 mM). Lastly, the AV IC_{50} value was calculated in the presence of 0.5 mM 4-NB plus 0.5 mM 4-HB. Under these conditions, the IC_{50} of AV increased significantly in comparison to that of parasites treated only with 0.5 mM 4-NB. Therefore, the competition of 4-NB with 4-HB suggests that the UQ biosynthesis is the target for 4-NB in the malaria parasite. This also highlights UQ biosynthesis as the possible mechanism through which 4-NB potentiates the antiplasmodial activity of AV (Fig. 8). The results discussed above were confirmed by flow cytometry (Fig. S5). Furthermore, by replacing AV with chloroquine (a typical antimalarial agent), no potentiation was observed due to the addition of 4-NB. This suggests that 4-NB effect is not general or nonspecific (see Fig. S5).

Oxygen consumption assays. Total cellular oxygen consumption (R′) was measured in erythrocyte-free parasites isolated from cultures treated or untreated for 48 h with 50 μM 4-NB. There were no significant differences in R' values between parasites

treated and untreated with 4-NB (see Fig. S7). Afterwards, AV was titrated and the differences in oxygen consumption were assessed in either untreated (Fig. 9a) or 4-NB-treated parasites (Fig. 9b). The oxygen consumption under particular AV concentrations was normalized to the corresponding R′ slope (Fig. 9c). The results indicate that the parasites pretreated with 50 μM 4-NB had greater sensitivity to specific AV concentrations (0 to 0.8 nM) (Fig. 9c). Note that at 50 μM, 4-NB did not affect parasitic growth or oxygen consumption (see Fig. 9d). In another experiment, the isolated schizonts were treated with progressive 4-NB concentrations during the oxygen consumption assay to assess the direct effects of 4-NB (Fig. 9d). Contrary to what was previously observed in human cells (26, 28), 4-NB reduced oxygen consumption at concentrations greater than 200 μM, which is suggestive of a direct effect on *P. falciparum* mitochondria at high concentrations. In all experiments, the inhibition of oxygen consumption in response to AV, as shown in Fig. 9b, was assessed to confirm that the oxygen consumption was linked to the electron transport system.

DISCUSSION

The precursors of plasmodial ubiquinone. Prenylquinones are hydrophobic substances associated with several processes, such as lipoperoxidation avoidance and participation in transmembrane redox chains. However, the process most extensively studied is mitochondrial electronic transport (18, 29–31). This study aimed to elucidate the UQ biosynthetic pathway in the malaria parasite and the mechanism of action of AV. Moreover, a proof-of-concept research was performed to improve the efficacy of AV through the inhibition of the UQ biosynthetic pathway. This study focused on schizont stages because de Macedo et al. have already showed that the highest metabolic labeling of UQs is observed at this stage. Furthermore, they also demonstrated that the proportion between the different UQ homologs does not change substantially during the intraerythrocytic stages (24). The RP-HPLC system used in this study could distinguish between the different parasitic UQ homologs, and by performing $NaBH_4$ reduction assays and radiolabeling uninfected erythrocytes, the absence of co-elution of parasitic UQs with other human/parasitic isoprenylated substances has been confirmed. At the beginning of this study, UQ-8/9 biosynthesis in *Plasmodium* had only been identified by radiolabeling/chromatographic techniques (23–25, 32), and here, their identities were also revealed by mass spectrometry.

The advantages of using radiolabeling techniques for the study of isoprenylated compounds in *Plasmodium* have been discussed previously (32). Our research gives novel labeling strategies, which can be applied in malaria parasites or in other cell systems. [^{14}C-U] Glc incorporation into UQ begins during glycolysis. Then, products of the glycolytic pathway become precursors of both MEP and shikimate pathways. Similarly, Cassera et al. in 2004 demonstrated the incorporation of [1-^{14}C] sodium acetate into parasitic UQs (33). [^{3}H] GGPP and [^{3}H] FPP moieties are condensed to 40- and 45-carbon polyprenyl pyrophosphates required to prenylate 4-HB. 3-Polyprenyl 4-HB undergoes several modifications, including SAM-mediated methylations. Notably, [^{3}H] GGPP, [methyl-^{3}H] SAM, [ring-^{14}C(U)] 4-HB, and [^{14}C] Glc appeared to be better incorporated into UQ-9, while [^{3}H] FPP appeared to be better incorporated into UQ-8. Different proportions of radioactive incorporation between both UQ homologs were previously observed by de Macedo et al. (24) by employing [^{3}H] IPP, [^{3}H] FPP, and [^{3}H] GGPP. The authors attributed this phenomenon to a different prenyl-synthase preference for different isoprenic chains. Finally, the incorporation of [methyl-^{3}H] SAM into UQs is indicative of SAM-mediated methylations, reactions which are typically catalyzed by UbiG and UbiE enzymes (18). Following the same logic, L-[Me-^{14}C^{3}H] methionine and L-[Me-$^{2}H_3$] methionine were used to demonstrate SAM-mediated methylations for the biosynthesis of plant and alga prenylquinones, respectively (34, 35).

In a recent study, Valenciano et al. attempted to identify the aromatic precursors of plasmodial UQs using several [^{13}C] aromatic metabolites. However, the authors did not succeed in labeling the UQs (36). In spite of all reported biochemical evidence of UQ biosynthesis in the parasite, including the incorporation of [ring-14C(U)] 4-HB (23) and

[^{3}H] isoprenic moieties (24), Valenciano et al. suggested that the parasite would biosynthesize UQ from an unknown aromatic precursor or incorporate it from the host (36). The results presented here indicate that the parasite relies on an endogenous UQ biosynthetic pathway. Furthermore, this pathway does not seem to differ from that of most organisms.

Assessment of the proportion of ubiquinone homologs. The first evidence for ubiquinone biosynthesis in the parasites was published by Schnell et al. (23). The authors incubated parasites with [ring-^{14}C(U)] 4-HB and observed a higher radiolabeling in UQ-8. Contrary to this, our results indicate a higher radiolabeling in UQ-9. Since Schnell et al. performed experiments in blood cultures of infected monkeys (*P. falciparum* and *P. knowlesi*), it was suggested that the proportion of UQ homologs could differ based on the culture conditions and the *Plasmodium* species used (23). With respect to this, we observed a significant shift in the proportion between UQ-8 and UQ-9 upon the introduction of different gaseous mixtures in the culture. These results seem to indicate that under microaerophilic conditions, UQ-9 biosynthesis is reduced. It will remain unknown at least for a while whether this phenomenon is attributed to the oxygen-dependent catalytic activity of UbiA or polyprenyltransferases/syntheses. Nevertheless, it seems reasonable that the modifications in UQ biosynthesis observed in *Plasmodium* could occur naturally to aid the adaptation of the parasite to different environments within vertebrate hosts with various oxygen levels. In fact, besides the classic malaria culture method, parasitic viability has been reported previously under microaerophilic environments (25), high oxygen levels (37), or atmospheric air (38, 39). Taking into consideration the natural ability of the parasite to modify its UQ biosynthesis, we suggest that changes in membrane lipid composition (40), or even in UQ biosynthesis *per se*, could be the mechanisms underlying AV resistance. Similar to our observations, Tonhosolo et al. previously compared menaquinone-4 and UQ biosynthesis in *P. falciparum* while cultivating the parasite under oxygen-poor environments or normal conditions. The authors also used [^{3}H] GGPP as a precursor and observed a sharp reduction in UQ biosynthesis owing to the lack of oxygen. However, Tonhosolo et al. did not distinguish between the different UQ homologs, nor did they study their redox state (25).

The reason that several pathogenic protozoa, including several *Plasmodium* species, possess two or three UQ homologs at variable proportions during different parasitic stages remains undetermined (41). In certain organisms, this is attributed to UQ formation that occurs via sequential elongation of the isoprenic side chain (42). In other organisms, the different homologs may be formed specifically for different functions (41–43). In fact, it has already been demonstrated that while highly nonpolar UQ homologs are more suitable for electron-transfer reactions, polar homologs are more suitable as oxidative radical scavengers, possibly owing to their lower solubility in lipid membranes (44).

Rescue of AV treatment and its effects on ubiquinone redox status. AV rescue assays were performed at 5 or 10 μM dUQ (a soluble synthetic analog of UQ) and UQ-10, the major UQ homologs in humans (18, 28). Notably, the UQ-10 concentration employed here was higher than that usually detected in human blood, which ranges approximately between 0.5 to 5 μM (based on data from the Human Metabolome Database site, http://www.hmdb.ca/. Last accessed in January 2020). Although UQ is a highly hydrophobic molecule, its incorporation from the exogenous environment has been reported previously in human fibroblasts cultivated *in vitro* (28). However, in *Plasmodium* only dUQ could protect the parasite from the effects of AV. Understandably, several factors can influence UQ incorporation into cells. However, the results presented here strongly suggest that UQ-10 from the host is not incorporated into the parasite's mitochondria or that UQ-10 is nonfunctional for its mitochondrial electron transport system. Therefore, while other studies do not confirm the contrary, it is suggested that the parasite relies on UQ biosynthesis.

It was questioned whether only a single UQ homolog could be involved in the respiratory process. For this, the mitochondrial complex III was inhibited through a short AV treatment and changes in the UQ redox state were assessed. In mammalian cells, different UQ homologs are localized differently in the mitochondria or in the plasma

membrane and the localization determines the UQ interaction with mitochondrial enzymes (45). However, in *Plasmodium*, the inhibition of mitochondrial complex III by AV affected the redox state of both UQ homologs, and therefore, both homologs may naturally interact with the components of the electron transport system. To the best of our knowledge, this is the first observation of an AV effect on UQ redox state in any pathogen, and the results confirmed the hypothesized mechanism of action of AV. Kaneshiro et al. in 2000 studied the effects of AV on UQ biosynthesis in *Pneumocystis jirovecii* (42). A triphasic dose-response was observed, with inhibition at 10 nM and then stimulation up to 0.2 μM AV, followed by inhibition at 1 μM. This phenomenon is thought to be related to an exotic UQ biosynthesis route that remains poorly understood (42).

Physiological and pharmacological inhibition of ubiquinone biosynthesis. As previously mentioned, in *P. falciparum*, the total biosynthesized UQ content available for DHODH activity is decreased in oxygen-poor environments, and under these conditions, the antiplasmodial activity of AV is enhanced. Since AV competes with UQH_2, a depletion of the UQ pool would facilitate the AV interaction with the mitochondrial complex III and the DHODH activity. The use of a UQ biosynthesis inhibitor was considered a biochemical strategy for exploring the dependence of AV efficacy on UQ biosynthesis. Since the discovery of its inhibitory activity in 2010 (26), 4-NB has become a powerful tool used to study the effects of UQ depletion, and its mechanism of action seems to be the inhibition of UbiA enzymes (26). It has been demonstrated that 4-NB inhibits UQ biosynthesis in considerably divergent organisms. In human fibroblasts, 3 to 4 mM 4-NB treatments efficiently inhibit UQ biosynthesis with low cytotoxic effects (28). The low toxicity of the compound should not be surprising because UQ was shown to possess an extended half-life in several plants and animal cells, which could even reach 100 h in specific tissues (46, 47). In *P. falciparum*, 4-NB demonstrated to decrease [^{3}H] GGPP incorporation into UQ. Moreover, its IC_{50} value increased significantly at 72 h in the presence of dUQ, pABA, or 4-HB. The same rescue phenomena were not observed at 48 h, because the reduction in UQ biosynthesis at this time could not significantly affect the UQ pool, as discussed later. Therefore, 4-NB possesses the ability to inhibit UQ biosynthesis, although it may also affect other processes that were beyond the scope of this study, such as folate metabolism or pABA/4-HB intracellular uptake.

All concentrations of 4-NB used here potentiated AV (FIC values $<$0.5). Moreover, 1 mM 4-NB treatment reduced the AV IC_{50} value by over 1,000-fold, a potentiation phenomenon similar to that induced by proguanil (11, 14). In the presence of both 4-NB and 4-HB, the AV IC_{50} value increased significantly with respect to that in parasites treated only with 4-NB. Therefore, it is likely that 4-NB competition with 4-HB for UQ biosynthesis is the mechanism that potentiates AV. Notably, the results revealed that 4-NB could enhance the effects of AV on parasitic growth and respiration even at concentrations at which the compound does not exert any antiplasmodial activity. Certain aspects of these observations can be discussed. Since UQ may have a long half-life in the parasite, its biosynthesis is suggested to be essential only in the absence of a residual pool that can be continuously redox-recycled. Therefore, by combining drugs, which inhibits the biosynthesis and redox recycling of UQs, the UQ pool available for DHODH activity would be diminished drastically, and consequently, drug potentiation would occur.

Contrary to what was demonstrated in mammal cells (26, 28), 4-NB affected oxygen consumption in the malaria parasite, which indicates that the compound can also directly affect mitochondrial functions, in addition to inhibiting UQ biosynthesis. Moreover, the effects of 4-NB on oxygen consumption suggest that the compound possesses a target different from that of proguanil (11, 15). Regardless of the mechanism of action of 4-NB, AV potentiation on parasitic growth occurs at 4-NB concentrations where the oxygen consumption is not affected.

In addition to 4-NB, the most studied compounds that may also affect UQ

biosynthesis are those that interfere with isoprenoids biosynthesis. Fosmidomycin is the best-studied inhibitor of the MEP pathway in the parasite. One could suggest that fosmidomycin would also potentiate AV. However, Wiesner et al. in 2002 showed a ΣFIC value >1 for fosmidomycin-AV (48). In addition, Cassera et al. in 2004 showed that the treatment of parasites with fosmidomycin poorly inhibits UQ biosynthesis. These findings cause the authors to suggest the presence of an alternative pathway for isoprenoid biosynthesis in the parasite (33). Similarly, Howe et al. in 2013 demonstrated that malaria parasites expressing a UQ-independent yeast DHODH were not more resistant to fosmidomycin. Since UQ is considered an essential component for the parasite, the results of Howe et al. may indicate that UQ biosynthesis is not considerably affected due to fosmidomycin treatment (49).

Furthermore, all isoprenoid inhibitors may interfere not only with UQ biosynthesis but also with the biosynthesis of several isoprenoids. This effect could be the explanation for the emergence of unsuspected drug relationships (50). Therefore, we concluded that the broad-range effect of these drugs makes it difficult to use them as tools for delimiting a pathway to be responsible for the AV potentiation. In spite of these, we would encourage other research groups to explore AV synergy with isoprenoid biosynthesis inhibitors, considering the possibility of significantly increasing their antimalarial activity.

In conclusion, several isoprenic/aromatic metabolites, including 4-HB, GGPP, FPP, SAM, and Glc, were observed to be precursors of UQ in *P. falciparum*. Therefore, it is suggested that UQ biosynthesis in the malaria parasite does not differ from that observed in most organisms. The inhibition of mitochondrial complex III by AV was observed to affect the redox states of both UQ-8 and UQ-9 homologs. The biological importance and drug target potential of UQ biosynthesis were further investigated. 4-NB effectively inhibited parasitic UQ biosynthesis and significantly potentiated the effects of AV in parasite proliferation and oxygen consumption. The potentiation of AV by 4-NB is a strategy that could serve as a novel pharmacological therapy for malaria and other AV-sensitive pathogenic diseases.

MATERIALS AND METHODS

Reagents and stock solutions. Radiolabeled precursors [1-(n)-^{3}H]-geranylgeranyl-PP triammonium salt ([1-(n)-^{3}H]-GGPP, 15 Ci/mmol), *S*-adenosyl-L-[methyl-^{3}H] methionine ([methyl-^{3}H] SAM, 82 Ci/mmol), and D-[U-^{14}C] glucose (D-[U-^{14}C] Glc, 310 mCi/mmol) were obtained from Amersham-Pharmacia Biotech (Buckinghamshire, UK), [ring-^{14}C(U)] 4-HB (350 mCi/mmol) from American Radiolabed chemicals (Saint Louis, Missouri, USA), and [1-(n)-^{3}H] farnesyl-PP triammonium salt ([1-(n)-^{3}H] FPP, 23 Ci/mmol) from Perkin Elmer (Waltham, Massachusetts, USA). RPMI 1640 medium and Albumax I (0.5%) were purchased from Thermo Fisher Scientific (Waltham, Massachusetts, USA). All HPLC grade solvents, $NaBH_4$, dUQ, UQ-8/9/10 standards, AV, chloroquine diphosphate salt, 4-NB, 4-HB, pABA, and other basic reagents not mentioned here were purchased from Sigma (St. Louis, Missouri, USA). SYBR green I nucleic acid gel stain was obtained from Life Technologies (Eugene, OR, USA). AV stock solution was prepared at 25 mM in dimethyl sulfoxide. 4-NB, pABA, and 4-HB were dissolved at the concentrations mentioned in complete RPMI medium, and the pH was adjusted to 7.4 using 10% sodium bicarbonate (wt/vol). A stock solution 100 mM 4-NB in ethanol was prepared for the oxygen consumption assays, and the pH was adjusted to 7.4 using NaOH. The following stock solutions were prepared as well: 20 mM dUQ in ethanol, 1 mM chloroquine in water, and 50 mM UQ-10 in dimethyl sulfoxide.

Culturing *P. falciparum* asexual stages. *P. falciparum* 3D7 was cultured *in vitro* following the Radfar et al. methodology using RPMI 1640 medium complemented with Albumax I (0.5%) (51), and a gaseous mixture of 5% CO_2, 5% O_2, and 90% N_2 was employed as a reference. However, for certain experiments, oxygen-free mixtures (5% CO_2 and 95% N_2) were used until the culture attained a chocolate-brown color (25) (see Fig. S1 in the supplemental material). All gaseous mixtures were purchased from Air Products Brasil LTDA (São Paulo, SP, Brazil). Culture synchronization was performed using 5% (wt/vol) D-sorbitol solution (52), and the parasitic stages and parasitemia were monitored by the microscopic observation of Giemsa-stained smears. To avoid contamination of the cultures, PCR for mycoplasma detection was performed regularly (53).

Metabolic labeling. For metabolic labeling, the following was added to the cultures with minimum 15% parasitemia: 3.125 μCi/ml [^{3}H] FPP or [^{3}H] GGPP, 2.5 μCi/ml [methyl-^{3}H] SAM, 6.25 μCi/ml D-[U-^{14}C] Glc, or 0.5 μCi/ml [ring-^{14}C(U)] 4-HB. Parasite-infected/uninfected erythrocytes were incubated with the appropriate radiolabeled precursor for 12 to 18 h before harvesting them at the schizont stage using a magnetic column. For metabolic labeling with D-[U-^{14}C] Glc, parasites were incubated for 2 h in glucose-free RPMI complete medium before the radioactive precursor in standard RPMI complete medium was added (33). The experiments using antimalarial drugs and at different oxygen saturations were

conducted by treating 1.5×10^9 infected red blood cells for 48 h prior to the purification of the parasites. As an exception, short treatments were also performed for AV. In this case, 3×10^9 radiolabeled infected red blood cells were purified using a magnetic column and suspended in 20 ml RPMI complete medium at 37°C. The cell suspension was then divided in two aliquots: AV was added to one at 10 nM final concentration and was not added to the other one. Both samples were incubated at 37°C for 10 min and centrifuged at $600 \times g$ for 5 min, and the pellet was analyzed.

Magnetic column separation. Cultures at the schizont stage were purified using a magnetic column (MACS separation column, Manual Cell Separation) (54). The retained schizonts were eluted by washing with RPMI complete medium. After centrifugation at $600 \times g$ for 5 min, the schizont-infected erythrocytes were collected and frozen in liquid nitrogen for further analysis or analyzed immediately.

Monitoring parasite growth. The antimalarial effects exerted by the compounds separately or in combination on parasitic growth were monitored with respect to the untreated control. Experiments employing reference gaseous mixture were performed in 96-well plates, while experiments employing oxygen-free gaseous mixture were performed in 25 cm^2 cell culture flasks. Trials begun at the ring stage (2% parasitemia, 2% hematocrit), and parasite growth was monitored after 48 or 72 h by SYBR green I DNA staining or flow cytometry, as indicated (see below). Results were confirmed by the observation of Giemsa-stained smears.

SYBR green I DNA staining. 100 μl of the culture was incubated in a 96-well cell plate in dark at room temperature after adding 100 μl of SYBR green I 2/10,000 (vol/vol) in lysis buffer (20 mM Tris [pH 7.5], 5 mM EDTA, 0.008% saponin [wt/vol], 0.08% Triton X-100 [vol/vol]) (55). Fluorescence was measured using a POLARstar Omega fluorometer (BMG Labtech, Ortenberg, Germany) with the excitation and emission bands centered at 485 and 530 nm, respectively. The fluorescence values of uninfected erythrocytes were subtracted from the values obtained for infected cells.

Flow cytometry. The infected erythrocytes were harvested by centrifugation and resuspended in a solution of 10 μg/ml ethidium bromide in PBS. After incubation for 20 min at 37°C, the red blood cells were washed, resuspended in PBS, and analyzed on a Guava Easycyte Flow Cytometer (Merck, Darmstadt, Germany).

Effects of single-drug treatment on parasitic development *in vitro*. The concentration of the compound at which parasitic growth decreases 50% (IC_{50}) was determined after 48 or 72 h (55). Briefly, the drug samples for each compound were prepared at several concentrations by serial dilution in RPMI complete medium. An untreated control and dimethyl sulfoxide (DMSO) controls were always included. The IC_{50} value was determined using the GraphPad Prism software. Inhibition of parasite growth was analyzed with respect to the logarithm of the concentration using nonlinear regression (dose-response slope/variable sigmoid equation). All experiments that monitored parasitic growth were performed at least thrice with three technical triplicates for each one, and the R-squared values (R^2) were calculated. Only experiments with an R^2 value >0.95 were considered.

Drug interaction studies. The IC_{50} value was calculated as previously described in the presence or absence of different compounds. Specifically, the IC_{50} value of AV was calculated at 48 h in the absence or presence of different concentrations of 4-NB, dUQ, or UQ-10. Alternatively, the IC_{50} value of 4-NB was calculated at 48 or 72 h in the absence or presence of 0.5 mM 4-HB, 0.5 mM pABA, or 10 μM dUQ. A solvent control and an untreated control were always included. The single-drug fractional inhibitory concentration value (FIC value) was calculated as IC_{50} value of AV in a combined solution/IC_{50} value of AV. Only experiments with an R^2 value >0.95 were considered for the drug interactions study, and an AV FIC value <0.5 was considered a drug potentiation phenomenon (14).

Ubiquinone extraction. The following protocol was adapted from Sussmann et al. (37). However, to avoid altering the UQ redox state, the use of butylated hydroxytoluene (BHT) was avoided. First, 1 ml deionized water was added to the infected red blood cells. The suspension was sonicated thrice for 10 s at 50-W pulses in ice and the proteins were precipitated by adding 400 μl ethanol/ml sample. The extraction was performed using 2 ml n-hexane/ml sample. The sample was homogenized for 1 min in a vortex and centrifuged at $2,700 \times g$ for 10 min at 4°C, and the supernatant was collected. This extractive procedure was repeated thrice, and the supernatants were combined and dried under a stream of nitrogen in a glass tube in the dark. The obtained material was then suspended in 200 μl of methanol/ethanol (7:3, vol/vol) containing internal standards of the UQ homologs to be studied.

Oxygen consumption assays. Oxygen consumption assays were adapted from Murphy et al. (56). Parasites at the trophozoite/young schizont stages were cultured in the absence or presence of 50 μM 4-NB for 48 h. Treated/untreated cultures were centrifuged ($1,500 \times g$ for 5 min at 4°C), washed with PBS, and lysed with 30 ml of 0.03% saponin in PBS at 25°C for 5 min. Parasite cultures were then centrifuged at $1,500 \times g$ for 5 min at 4°C and subsequently washed in respiration buffer (125 mM sucrose, 65 mM KCl, 5 mM L-glutamine, 10 mM HEPES-KOH [pH 7.2], 5 mM $MgCl_2$, 2 mM KH_2PO_4, 0.5 mM EGTA). The samples were then resuspended in incomplete culture medium (RPMI 1640 medium without Albumax I) at 1×10^9 cells/ml and the oxygen uptake was measured immediately at 37°C using a high-resolution oxygraph (Oxygraph-2k Oroborus Instruments, Innsbruck, Austria). The total cellular oxygen consumption (R′) was then recorded. Then, the AV titration was performed with successive additions of 1 μl of AV from the stock sample (400 nM in ethanol) by waiting at least 4 min between additions. The total inhibition of the respiration could be demonstrated after reaching a final concentration of approximately 0.8 nM AV. Alternatively, a 4-NB titration was performed with successive additions of 4-NB from the stock solution (100 mM in ethanol). The total inhibition of the respiration in this case could be demonstrated after reaching a final concentration of approximately 2 mM 4-NB.

Reverse phase-high performance liquid chromatography (RP-HPLC). The RP-HPLC assays were adapted from Jemiota-Rzemińska et al. (57). In all experiments, both UQ-8/9 standards were co-injected

in the sample to determinate the exact retention time. The retention time for each UQH_2 was determined separately by reducing the UQ standards in ethanol. The system was operated at 30°C using methanol/ethanol (7:3 vol/vol) as mobile phase at a flow rate of 1.2 ml/min. The Phenomenex Luna C18 column (250 mm by 4.6 mm by 5 μm) (Phenomenex, CA, USA) coupled to a Phenomenex precolumn C18 was used as the stationary phase. Data were recorded using a Diode Arrangement Detector Gilson170 operating at 275 nm for UQs and at 290 nm for UQH_2. The software used for data processing was Unipoint LC (Gilson). The fractions were collected using a fraction collector FC203B at 45-s or 60-s intervals, as indicated for each experiment (Gilson, Villiers-le-Bel, France). For radiation monitoring, the fractions were dried at 50°C, suspended in 0.5 ml of liquid scintillation mixture (PerkinElmer Life Sciences, MA, USA), and analyzed with a Beckman LS 5000 TD β-counter apparatus (Beckman, CA, USA). The metabolic profiles were analyzed with the OriginPro 8.1 software (OriginLab Corporation, MA, USA) using bars or spline-connected point graphs.

$NaBH_4$ reduction assays. The $NaBH_4$ reduction assays were used to study the redox state of parasitic UQs as well as to assess the quality of the chromatographic method described previously. For this, UQ commercial standards or parasitic [^{3}H] UQ purified by RP-HPLC and dried under a nitrogen stream were employed. In both cases, UQ was suspended in 200 μl ethanol, a few granules of $NaBH_4$ were added, and the samples were immediately analyzed by RP-HPLC (58).

Liquid chromatography-mass spectrometry (LC-MS). Approximately 1×10^{10} erythrocyte-free schizonts were obtained by resuspending the red blood cells in a lysis solution (PBS containing 0.1% saponin plus 2g/liter Glc) at a proportion of 0.5 ml erythrocytes/30 ml lysis solution. The samples were centrifuged at 3,300 $\times$ *g* for 7 min at 4°C and washed twice with 30 ml PBS plus 2 g/liter Glc. The UQ extraction procedure was performed as previously described, and the dried residues were suspended in 100 μl of methanol/$CHCl_3$ (7:3, vol/vol). An LC-MS system from Thermo Scientific consisting of an ACCELA 600 quaternary pump, an ACCELAAS autosampler, and a triple quadrupole mass spectrometer TSQ Quantum Max were used for UQ-8 ($C_{54}H_{82}O_4$) and UQ-9 ($C_{59}H_{90}O_4$) identification. The separation procedure was performed using a Kinetex phenyl-hexyl analytical column (2.1 by 50 mm, 5 μm) at 200 μl/min by isocratic elution with the following mobile phases: A, isopropanol/methanol (60:40, vol/vol) with 5 mM ammonium acetate and B, methanol/water (50:50, vol/vol). The triple quadrupole mass spectrometer TSQ Quantum Max was operated at positive polarity and the ionization conditions were 220°C capillary temperature, 371°C vaporizer temperature, 5,000 V spray voltage, 30 arb (arbitrary units) sheath gas pressure, 45 arb auxiliary gas pressure, 117 V tube lens offset, and 8 V skimmer offset. To achieve the highest sensitivity and selectivity, the mass spectrometer was operated in the MRM mode for monitoring transitions in each prenylquinone residue using a collision gas pressure of 1.5 mTorr and collision energy of 24 eV. The MRM transitions were 728 to 197 for UQ-8 and 796 to 197 for UQ-9.

SUPPLEMENTAL MATERIAL

Supplemental material is available online only.

SUPPLEMENTAL FILE 1, PDF file, 0.7 MB.

ACKNOWLEDGMENTS

I.B.V., M.C., C.A.Z., N.L.B., and R.A.C.S. are fellows from the Conselho Nacional de Desenvolvimento Científico e Tecnológico (CNPq) and Fundação de Amparo à Pesquisa do Estado de São Paulo (FAPESP). This work was supported by FAPESP (process number 2017/22452-1 awarded to A.M.K. and 2015/19316-3 and 2018/12589-2 awarded to M.F. A.), Coordenação de Aperfeiçoamento de Pessoal de Nível Superior (CAPES), and CNPq. We thank FAPESP, CNPq, and CAPES for the financial support. We thank William Tadeu Lara Festuccia and Érique de Castro from the Laboratório de Fisiologia Molecular e Metabolismo in ICB/USP, for providing the platform and helping with oximetry and Sírio Libanês Hospital (NESTA, São Paulo, Brazil) for generously providing the erythrocytes.

All the authors certify that they have no conflicts of interest.

REFERENCES

1. World Health Organization. 2019. World Malaria Report. Geneva. https://www.who.int/publications/i/item/9789241565721.
2. Mills A, Lubell Y, Hanson K. 2008. Malaria eradication: the economic, financial and institutional challenge. Malar J 7:S11. https://doi.org/10.1186/1475-2875-7-S1-S11.
3. White NJ. 1998. Preventing antimalarial drug resistance through combinations. Drug Resist Updat 1:3–9. https://doi.org/10.1016/S1368-7646(98)80208-2.
4. Vaidya AB, Mather MW. 2009. Mitochondrial evolution and functions in malaria parasites. Annu Rev Microbiol 63:249–267. https://doi.org/10.1146/annurev.micro.091208.073424.
5. Müller S. 2004. Redox and antioxidant systems of the malaria parasite *Plasmodium falciparum*. Mol Microbiol 53:1291–1305. https://doi.org/10.1111/j.1365-2958.2004.04257.x.
6. Scheibel LW, Ashton SH, Trager W. 1979. *Plasmodium falciparum*: microaerophilic requirements in human red blood cells. Exp Parasitol 47:410–418. https://doi.org/10.1016/0014-4894(79)90094-8.
7. Torrentino-Madamet M, Desplans J, Travaillé C, James Y, Parzy D. 2010. Microaerophilic respiratory metabolism of *Plasmodium falciparum* mitochondrion as a drug target. Curr Mol Med 10:29–46. https://doi.org/10.2174/156652410791065390.
8. van Dooren GG, Stimmler LM, McFadden GI. 2006. Metabolic maps and

functions of the *Plasmodium* mitochondrion. FEMS Microbiol Rev 30:596–630. https://doi.org/10.1111/j.1574-6976.2006.00027.x.
9. Haile LG, Flaherty JF. 1993. Atovaquone: a review. Ann Pharmacother 27:1488–1494. https://doi.org/10.1177/106002809302701215.
10. Balabaskaran Nina P, Morrisey JM, Ganesan SM, Ke H, Pershing AM, Mather MW, Vaidya AB. 2011. ATP synthase complex of *Plasmodium falciparum*: dimeric assembly in mitochondrial membranes and resistance to genetic disruption. J Biol Chem 286:41312–41322. https://doi.org/10.1074/jbc.M111.290973.
11. Painter HJ, Morrisey JM, Mather MW, Vaidya AB. 2007. Specific role of mitochondrial electron transport in blood-stage *Plasmodium falciparum*. Nature 446:88–91. https://doi.org/10.1038/nature05572.
12. Ke H, Morrisey JM, Ganesan SM, Painter HJ, Mather MW, Vaidya AB. 2011. Variation among *Plasmodium falciparum* strains in their reliance on mitochondrial electron transport chain function. Eukaryot Cell 10:1053–1061. https://doi.org/10.1128/EC.05049-11.
13. Vaidya AB, Mather MW. 2000. Atovaquone resistance in malaria parasites. Drug Resist Updat 3:283–287. https://doi.org/10.1054/drup.2000.0157.
14. Canfield CJ, Pudney M, Gutteridge WE. 1995. Interactions of atovaquone with other antimalarial drugs against *Plasmodium falciparum* in vitro. Exp Parasitol 80:373–381. https://doi.org/10.1006/expr.1995.1049.
15. Srivastava IKK, Vaidya ABB. 1999. A mechanism for the synergistic antimalarial action of atovaquone and proguanil. Antimicrob Agents Chemother 43:1334–1339. https://doi.org/10.1128/AAC.43.6.1334.
16. Carrington HC, Crowther AF, Davey DG, Levi AA, Rose FL. 1951. A metabolite of paludrine with high antimalarial activity. Nature 168:1080. https://doi.org/10.1038/1681080a0.
17. Pécoul B, Chirac P, Trouiller P, Pinel J. 1999. Access to essential drugs in poor countries: a lost battle? JAMA 281:361–367. https://doi.org/10.1001/jama.281.4.361.
18. Verdaguer IB, Zafra CA, Crispim M, Sussmann RAC, Kimura EA, Katzin AM. 2019. Prenylquinones in human parasitic protozoa: biosynthesis, physiological functions, and potential as chemotherapeutic targets. Molecules 24:3721. https://doi.org/10.3390/molecules24203721.
19. Jordão FM, Kimura EA, Katzin AM. 2011. Isoprenoid biosynthesis in the erythrocytic stages of *Plasmodium falciparum*. Mem Inst Oswaldo Cruz 106(Suppl):134–141. https://doi.org/10.1590/S0074-02762011000900018.
20. Hyde JE. 2005. Exploring the folate pathway in *Plasmodium falciparum*. Acta Trop 94:191–206. https://doi.org/10.1016/j.actatropica.2005.04.002.
21. Taylor AE. 1957. The effect of paraminobenzoic acid, parahydroxybenzoic acid and riboflavin on *Plasmodium gallinaceum* in chicks. Trans R Soc Trop Med Hyg 51:241–247. https://doi.org/10.1016/0035-9203(57)90023-8.
22. Zhang Y, Merali S, Meshnick SR. 1992. p-Aminobenzoic acid transport by normal and *Plasmodium falciparum*-infected erythrocytes. Mol Biochem Parasitol 52:185–194. https://doi.org/10.1016/0166-6851(92)90051-K.
23. Schnell JV, Siddiqui WA, Geiman QM. 1971. Biosynthesis of coenzymes Q by malarial parasites. 2. Coenzyme Q synthesis in blood cultures of monkeys infected with malarial parasites (*Plasmodium falciparum* and *P. knowlesi*). J Med Chem 14:1026–1029. https://doi.org/10.1021/jm00293a002.
24. de Macedo CS, Uhrig ML, Kimura EA, Katzin AM. 2002. Characterization of the isoprenoid chain of coenzyme Q in *Plasmodium falciparum*. FEMS Microbiol Lett 207:13–20. https://doi.org/10.1111/j.1574-6968.2002.tb11021.x.
25. Tonhosolo R, Gabriel HB, Matsumura MY, Cabral FJ, Yamamoto MM, D'Alexandri FL, Sussmann RAC, Belmonte R, Peres VJ, Crick DC, Wunderlich G, Kimura EA, Katzin AM. 2010. Intraerythrocytic stages of *Plasmodium falciparum* biosynthesize menaquinone. FEBS Lett 584:4761–4768. https://doi.org/10.1016/j.febslet.2010.10.055.
26. Forsman U, Sjöberg M, Turunen M, Sindelar PJ. 2010. 4-Nitrobenzoate inhibits coenzyme Q biosynthesis in mammalian cell cultures. Nat Chem Biol 6:515–517. https://doi.org/10.1038/nchembio.372.
27. Nowicka B, Kruk J. 2016. Cyanobacteria use both p-hydroxybenzoate and homogentisate as a precursor of plastoquinone head group. Acta Physiol Plant 38:49. https://doi.org/10.1007/s11738-015-2043-0.
28. Quinzii CM, Tadesse S, Naini A, Hirano M. 2012. Effects of inhibiting CoQ10 biosynthesis with 4-nitrobenzoate in human fibroblasts. PLoS One 7:e30606. https://doi.org/10.1371/journal.pone.0030606.
29. Holsclaw CM, Sogi KM, Gilmore SA, Schelle MW, Leavell MD, Bertozzi CR, Leary JA. 2008. Structural characterization of a novel sulfated menaquinone produced by *stf3* from *Mycobacterium tuberculosis*. ACS Chem Biol 3:619–624. https://doi.org/10.1021/cb800145r.
30. Biswas S, Haque R, Bhuyan NR, Bera T. 2008. Participation of chlorobiumquinone in the transplasma membrane electron transport system of Leishmania donovani promastigote: effect of near-ultraviolet light on the redox reaction of plasma membrane. Biochim Biophys Acta 1780:116–127. https://doi.org/10.1016/j.bbagen.2007.09.006.
31. Nandi N, Bera T, Kumar S, Purkait B, Kumar A, Das P. 2011. Involvement of thermoplasmaquinone-7 in transplasma membrane electron transport of Entamoeba histolytica trophozoites: a key molecule for future rational chemotherapeutic drug designing. J Bioenerg Biomembr 43:203–215. https://doi.org/10.1007/s10863-011-9347-6.
32. Kimura EA, Wunderlich G, Jordão FM, Tonhosolo R, Gabriel HB, Sussmann RAC, Saito AY, Katzin AM. 2011. Use of radioactive precursors for biochemical characterization the biosynthesis of isoprenoids in intraerythrocytic stages of *Plasmodium falciparum*., p 27–46. *In* Singh N, Radioisotopes: Applications in Bio-Medical Science. IntechOpen.
33. Cassera MB, Gozzo FC, D'Alexandri FL, Merino EF, del Portillo HA, Peres VJ, Almeida IC, Eberlin MN, Wunderlich G, Wiesner J, Jomaa H, Kimura EA, Katzin AM. 2004. The methylerythritol phosphate pathway is functionally active in all intraerythrocytic stages of *Plasmodium falciparum*. J Biol Chem 279:51749–51759. https://doi.org/10.1074/jbc.M408360200.
34. Threlfall DR, Whistance GR, Goodwin TW. 1968. Biosynthesis of phytoquinones. Incorporation of L-[Me-^{14}C,3H]methionine into terpenoid quinones and chromanols in maize shoots. Biochem J 106:107–112. https://doi.org/10.1042/bj1060107.
35. Threlfall DR. 1972. Incorporation of L-(Me- 2 H 3) methionine into isoprenoid quinones and related compounds by Euglena gracilis. Biochim Biophys Acta1972/11/30 280:472–480. https://doi.org/10.1016/0005-2760(72)90255-X.
36. Valenciano AL, Fernández-Murga ML, Merino EF, Holderman NR, Butschek GJ, Shaffer KJ, Tyler PC, Cassera MB. 2019. Metabolic dependency of chorismate in *Plasmodium falciparum* suggests an alternative source for the ubiquinone biosynthesis precursor. Sci Rep 9:13936. https://doi.org/10.1038/s41598-019-50319-5.
37. Sussmann RAC, Angeli CB, Peres VJ, Kimura EA, Katzin AM. 2011. Intraerythrocytic stages of *Plasmodium falciparum* biosynthesize vitamin E. FEBS Lett 585:3985–3991. https://doi.org/10.1016/j.febslet.2011.11.005.
38. Branco A, Francisco D, Hanscheid T. 2018. Is there a "normal" oxygen concentration for in vitro *Plasmodium* cultures? Trends Parasitol 34:811–812. https://doi.org/10.1016/j.pt.2018.07.003.
39. Mirovsky P. 1989. Continuous culture of *Plasmodium falciparum* asexual stages in "normal" air atmosphere. Folia Parasitol (Praha) 36:107–112.
40. Cauchetier E, Loiseau PMM, Lehman J, Rivollet D, Fleury J, Astier A, Deniau M, Paul M. 2002. Characterisation of atovaquone resistance in *Leishmania infantum* promastigotes. Int J Parasitol 32:1043–1051. https://doi.org/10.1016/S0020-7519(02)00065-6.
41. Ellis JE. 1994. Coenzyme Q homologs in parasitic protozoa as targets for chemotherapeutic attack. Parasitol Today 10:296–301. https://doi.org/10.1016/0169-4758(94)90079-5.
42. Kaneshiro ES, Sul D, Hazra B. 2000. Effects of atovaquone and diospyrin-based drugs on ubiquinone biosynthesis in *Pneumocystis carinii* organisms. Antimicrob Agents Chemother 44:14–18. https://doi.org/10.1128/aac.44.1.14-18.2000.
43. Ellis JE, Wyder MA, Zhou L, Gupta A, Rudney H, Kaneshiro ES. 1996. Composition of *Pneumocystis carinii* neutral lipids and identification of coenzyme Q10 as the major ubiquinone homolog. J Eukaryot Microbiol 43:165–170. https://doi.org/10.1111/j.1550-7408.1996.tb01385.x.
44. Kagan VE, Serbinova EA, Koynova GM, Kitanova SA, Tyurin VA, Stoytchev TS, Quinn PJ, Packer L. 1990. Antioxidant action of ubiquinol homologues with different isoprenoid chain length in biomembranes. Free Radic Biol Med 9:117–126. https://doi.org/10.1016/0891-5849(90)90114-x.
45. Nowicka B, Kruk J. 2010. Occurrence, biosynthesis and function of isoprenoid quinones. Biochim Biophys Acta 1797:1587–1605. https://doi.org/10.1016/j.bbabio.2010.06.007.
46. Wanke M, Swiezewska E, Dallner G. 2000. Half-life of ubiquinone and plastoquinone in spinach cells. Plant Sci 154:183–187. https://doi.org/10.1016/s0168-9452(00)00200-4.
47. Thelin A, Schedin S, Dallner G. 1992. Half-life of ubiquinone-9 in rat tissues. FEBS Lett 313:118–120. https://doi.org/10.1016/0014-5793(92)81425-l.
48. Wiesner J, Henschker D, Hutchinson DB, Beck E, Jomaa H. 2002. *In vitro* and *in vivo* synergy of fosmidomycin, a novel antimalarial drug, with clindamycin. Antimicrob Agents Chemother 46:2889–2894. https://doi.org/10.1128/aac.46.9.2889-2894.2002.
49. Howe R, Kelly M, Jimah J, Hodge D, Odom AR. 2013. Isoprenoid biosynthesis inhibition disrupts Rab5 localization and food vacuolar integrity in *Plasmodium falciparum*. Eukaryot Cell 12:215–223. https://doi.org/10.1128/EC.00073-12.
50. da Silva MF, Saito AY, Peres VJ, Oliveira AC, Katzin AM. 2015. *In vitro* antimalarial activity of different inhibitors of the plasmodial isoprenoid

synthesis pathway. Antimicrob Agents Chemother 59:5084–5087. https://doi.org/10.1128/AAC.04161-14.
51. Radfar A, Méndez D, Moneriz C, Linares M, Marín-García P, Puyet A, Diez A, Bautista JM. 2009. Synchronous culture of *Plasmodium falciparum* at high parasitemia levels. Nat Protoc 4:1899–1915. https://doi.org/10.1038/nprot.2009.198.
52. Lambros C, Vanderberg JP. 1979. Synchronization of *Plasmodium falciparum* erythrocytic stages in culture. J Parasitol 65:418–420. https://doi.org/10.2307/3280287.
53. Rowe JA, Scragg IG, Kwiatkowski D, Ferguson DJ, Carucci DJ, Newbold CI. 1998. Implications of mycoplasma contamination in *Plasmodium falciparum* cultures and methods for its detection and eradication. Mol Biochem Parasitol 92:177–180. https://doi.org/10.1016/s0166-6851(97)00237-5.
54. Ribaut C, Berry A, Chevalley S, Reybier K, Morlais I, Parzy D, Nepveu F, Benoit-Vical F, Valentin A. 2008. Concentration and purification by magnetic separation of the erythrocytic stages of all human *Plasmodium* species. Malar J 7:45. https://doi.org/10.1186/1475-2875-7-45.
55. Smilkstein M, Sriwilaijaroen N, Kelly JX, Wilairat P, Riscoe M. 2004. Simple and inexpensive fluorescence-based technique for high-throughput antimalarial drug screening. Antimicrob Agents Chemother 48:1803–1806. https://doi.org/10.1128/aac.48.5.1803-1806.2004.
56. Murphy AD, Doeller JE, Hearn B, Lang-Unnasch N. 1997. *Plasmodium falciparum*: cyanide-resistant oxygen consumption. Exp Parasitol 87:112–120. https://doi.org/10.1006/expr.1997.4194.
57. Jemiota-Rzemińska M, Latowski D, Strzałka K. 2001. Incorporation of plastoquinone and ubiquinone into liposome membranes studied by HPLC analysis. The effect of side chain length and redox state of quinone. Chem Phys Lipids 110:85–94. https://doi.org/10.1016/s0009-3084(00)00227-9.
58. Yoshida K, Shibata M, Terashima I, Noguchi K. 2010. Simultaneous determination of in vivo plastoquinone and ubiquinone redox states by HPLC-based analysis. Plant Cell Physiol 51:836–841. https://doi.org/10.1093/pcp/pcq044.